The magnitude of strength of the proximal femur under a certain loading condition differs depending on the bone density distribution and morphology of each individual patient. To evaluate fracture risk in each patient, it is ideal to analyze strengths under all loading conditions occurring in the activities of daily living. However, it takes a large amount of time to carry out predictions as a screening using CT/FEM under many circumstances. One of the solutions to this problem is to find the typical loading direction that correlates with other conditions. For this reason, we investigated the correlation among multiple loading conditions. The correlation between predicted fracture loads in SC and those in each FC was significant but weak, with a correlation coefficient of 0.467–0.631. To evaluate strength of the proximal femur in each individual patient, both strength under SC and strength under FC should be assessed. The correlations of the predicted strength among FC2, FC3, and FC4 were relatively high with correlation coefficients of 0.728 to 0.894. Upon further analysis of these conditions, the correlation coefficients were even higher with 0.894 between FC3 and FC2 and 0.861 between FC3 and FC4. Thus, FC3 was thought to be representative of FC2 and FC4. Conversely, the predicted strength under FC1 had poor correlations between FC2, FC3, and FC4 with coefficients of 0.586, 0.584, and 0.463 respectively. Thus, it was concluded that the strength under FC1 should be evaluated independently.

In all FCs except FC1, only trochanteric fractures were predicted. However, in FC1, both neck and trochanteric fractures were predicted. Hirsch and Frankel [17] reported that compressive force along the long axis of the neck is necessary to cause femoral neck fracture. Femoral neck angle is reportedly 120–130° [18]. FC1 may thus be able to cause femoral neck fractures. Fujii also reported that FC1 generated neck fractures and that this does not contradict the results of previous studies [6]. Hall et al. reported that the difference in bone density between the right and left femora as measured by dual X-ray absorptiometry was within 5% and that it was sufficient for measuring either side of the femur to evaluate osteoporosis [19]. Boston [20] reported that in 83% of the patients with previous hip fracture who sustained another hip fracture on the contralateral side, the fracture type agreed well with the previous one. If morphological differences between both sides of the femur are assumed to be absent, loading direction alone appears to represent the decisive factor for fracture type under all FCs except FC1. However, the different fracture type in FC1 could be generated by differences in morphology of the proximal femur in each individual patient.

Ford et al. [7] and Keyak et al. [8] investigated the influence of load direction on strength of the proximal femur. Ford et al. and Keyak et al. reported that the predicted strength by CT/FEM tended to decrease as the loading direction shifted from lateral to posterolateral. This was not contradictory to our findings. However, the analytical method adopted in those studies was a linear finite element method and the number of analyzed materials was only one sample in the study by Ford et al. and four samples in the study by Kayak et al. For this reason, they did not conduct the statistical analysis that we did. In addition, neither of these studies evaluated fracture site or type.

The load and boundary conditions adopted in the present study did not include muscle forces or reaction forces generated from ligamentous attachments. In addition, analyses utilized static mechanics rather than impact mechanics. Shock absorption by the soft tissues of patients was not taken into account [21]. Conditions in the simulation thus differed from those in actual settings. However, the load and boundary conditions adopted in the study were thought to reflect actual conditions, as simulated fractures resembled those sustained by the subjects. Further investigation adopting more realistic conditions is necessary, to take into account muscle forces and reaction forces from ligaments. Another limitation in this particular simulation technique was the inability to deal with large deformation of the model, from which refracture of bone fragments by collision could be simulated. The current method could only detect the initial failure site of the element under small deformation of the model, as although the results showed that fracture type could be judged even using this technique.

Previous studies have investigated the strengths of specimens ex vivo, whereas our study investigated strengths of the proximal femur in patients. In CT of the proximal femur in patients, images may have been deteriorated due to the influence of the pelvis or soft tissues nearby. Accuracy of strength prediction in vivo using a CT-based FE method could thus be impaired. Keyak and Falkinstein compared predicted strengths using a CT-based FE method from CT data obtained from two cadaveric specimens in situ to those from the same specimens in vitro [22]. Prediction from in situ specimens was found to overestimate strength by 8–13%. Although our study adopted a different simulation method from that of Keyak et al., our results might still have overestimated strength. However, our simulation method minimized partial volume effects by using triangular elements on the outer surface of the model. In addition, bone mineral density in tetrahedral elements was determined from mean value in Hounsfield units at 17 points within the element, to accurately simulate the distribution of bone mineral density even when the quality of CT data might have been deteriorated.

Our aim was to provide a quantitative diagnostic tool to accurately evaluate bone fracture risk by taking as many determinant factors for bone strength as possible into consideration. The CT-based FEM is the most advanced method to satisfy these demands. Our intention was not to provide a method to decide whether a bone in a certain patient would break under a certain mechanical environment. Instead, our approach involved the virtual extraction of a bone of interest from a patient and examining it under virtual static mechanical testing. The predicted strength from this simulation may be far from accurate in comparison to that derived from more realistic simulations incorporating dynamic analyses or more realistic mechanics incorporating geometrical rigidity/nonlinearity. Despite these limitations, the CT-based FEM offers a far more advanced method to diagnose bone fragility than the prevailing clinically available bone densitometry. Our model predicts elements where failure initiates, but does not take large deformation/geometrical nonlinearity into consideration. Our previous study verifying the accuracy of predicted fracture site by FEM simulation disclosed that the predicted fracture sites agreed well with the experimental fracture sites [9]. In the future, we intend to adopt more advanced simulation methods, including dynamic analyses or buckling simulations incorporating large deformation analyses or analyses with geometrical rigidity/nonlinearity.

To investigate the discrimination power of the CT/FEM, it is necessary to conduct a case-controlled study investigating the sensitivity and specificity of the CT/FEM by comparing the predicted strengths between patients with fractures and patients without fractures. However, the present study was not aimed at investigating the above issues. We clarified the loading directions that are vulnerable to fracture in the patients with hip fracture and the results were not contradictory to those of previous studies. Because a case-controlled study involving patients without fractures is also proceeding in our department, the results from this comparative study will soon be reported. If we could identify the loading directions under which the proximal femur is most vulnerable to fracture, more effective means of preventing fracture might be identified. With such knowledge, shape or attachment site of hip protectors could be optimized to maximize fracture prevention [23]. Likewise, motion exercises could be provided for elderly individuals to avoid falls in the most risky directions. The current investigation could contribute to the acquisition of useful knowledge allowing the establishment of more efficacious means of preventing hip fractures.

Acknowledgments

This work was funded by a grant in aid for Scientific Research received from the Japan Society for the Promotion of Science (14657356).

References

[1] Yoshimura N, Suzuki T, Hosoi T, Orimo H. Epidemiology of hip fracture in Japan: incidence and risk factors. J Bone Miner Metab 2005;23:78–80 Suppl.
[2] Hedlund R, Lindgren U. Trauma type, age, and gender as determinants of hip fracture. J Orthop Res 1987;5:242–6.
[3] Cummings SR, Black DM, Nevitt MC, Browner WS, Cauley JA, Genant HK, et al. Appendicular bone density and age predict hip fracture in women. The Study of Osteoporotic Fractures Research Group. JAMA 1990;263:665–8.
[4] Sloan J, Holloway G. Fractured neck of the femur: the cause of the fall? Injury 1981;13:230–2.
[5] Pinilla TP, Boardman KC, Bouxsein ML, Myers ER, Hayes WC. Impact direction from a fall influences the failure load of the proximal femur as much as age-related bone loss. Calcif Tissue Int 1996;58:231–5.
[6] Fujii M. Experimental study on the mechanism of femoral neck fractures. Nippon Seikeigeka Gakkai Zasshi 1987;61:531–41.
[7] Ford CM, Keaveny TM, Hayes WC. The effect of impact direction on the structural capacity of the proximal femur during falls. J Bone Miner Res 1996;11: 377–83.
[8] Keyak JH, Skinner HB, Fleming JA. Effect of force direction on femoral fracture load for two types of loading conditions. J Orthop Res 2001;19:539–44.
[9] Bessho M, Ohnishi I, Matsuyama J, Matsumoto T, Imai K, Nakamura K. Prediction of strength and strain of the proximal femur by a CT-based finite element method. J Biomech 2007;40:1745–53.
[10] Ito M, Lang TF, Jergas M, Ohki M, Takada M, Nakamura T, et al. Spinal trabecular bone loss and fracture in American and Japanese women. Calcif tissue int 1997;61: 123–8.
[11] Keyak JH, Kaneko TS, Rossi SA, Pejcic MR, Tehranzadeh J, Skinner HB. Predicting the strength of femoral shafts with and without metastatic lesions. Clin Orthop Relat Res 2005;439:161–70.
[12] Keyak JH, Kaneko TS, Tehranzadeh J, Skinner HB. Predicting proximal femoral strength using structural engineering models. Clin Orthop Relat Res 2005:219–28.
[13] Keyak JH, Rossi SA, Jones KA, Skinner HB. Prediction of femoral fracture load using automated finite element modeling. J Biomech 1998;31:125–33.
[14] Keller TS. Predicting the compressive mechanical behavior of bone. J Biomech 1994;27:1159–68.
[15] Bayraktar HH, Morgan EF, Niebur GL, Morris GE, Wong EK, Keaveny TM. Comparison of the elastic and yield properties of human femoral trabecular and cortical bone tissue. J Biomech 2004;37:27–35.
[16] McCalden RW, McGeough JA, Barker MB, Court-Brown CM. Age-related changes in the tensile properties of cortical bone. The relative importance of changes in porosity, mineralization, and microstructure. J Bone Joint Surg 1993;75-A: 1193–205.
[17] Hirsch C, Frankel VH. Analysis of forces producing fractures of the proximal end of the femur. J Bone Joint Surg Br 1960;42:633–40.
[18] Anderson JY, Trinkaus E. Patterns of sexual, bilateral and interpopulational variation in human femoral neck-shaft angles. J Anat 1998;192(Pt 2):279–85.
[19] Hall ML, Heavens J, Ell PJ. Variation between femurs as measured by dual energy X-ray absorptiometry (DEXA). Eur J Nucl Med 1991;18:38–40.
[20] Boston DA. Bilateral fractures of the femoral neck. Injury 1982;14:207–10.
[21] Robinovitch SN, McMahon TA, Hayes WC. Force attenuation in trochanteric soft tissues during impact from a fall. J Orthop Res 1995;13:956–62.
[22] Keyak JH, Falkinstein Y. Comparison of in situ and in vitro CT scan-based finite element model predictions of proximal femoral fracture load. Med Eng Phys 2003;25:781–7.
[23] Wiener SL, Andersson GB, Nyhus LM, Czech J. Force reduction by an external hip protector on the human hip after falls. Clin Orthop 2002:157–68.

SPINE Volume 34, Number 14, pp 1464–1469

Prediction of Vertebral Strength Under Loading Conditions Occurring in Activities of Daily Living Using a Computed Tomography-Based Nonlinear Finite Element Method

Takuya Matsumoto, MD,* Isao Ohnishi, MD, PhD,* Masahiko Bessho, MD, PhD,* Kazuhiro Imai, MD, PhD,*† Satoru Ohashi, MD,* and Kozo Nakamura, MD, PhD*

Study Design. A clinical study on osteoporotic vertebral strength in daily living using a computed tomography (CT)-based nonlinear finite element (FE) model.

Objective. To evaluate the differences in predicted fracture strength of osteoporotic vertebral bodies among the different loading conditions that are occurring in the activities of daily living.

Summary of Background Data. FE model has been reported to predict vertebral strength in uniaxial loading, but forward bending load plays an important role in osteoporotic vertebral fractures.

Methods. Strengths of the second lumbar vertebra in 41 female patients with postmenopausal osteoporosis were analyzed using a nonlinear CT-based FE method. Three different loading conditions were adopted uniaxial compression, forward bending, and erect standing. The same boundary condition was used for all loading conditions. Predicted strengths under forward bending and erect standing were compared with that under uniaxial compression and differences in strength were statistically analyzed.

Results. The regression equation relating strength under uniaxial compression to that under erect standing was expressed as $y = 0.8912x + 19.332$ ($R = 0.9522$), whereas the equation relating uniaxial compression to forward bending was $y = 0.7033x + 55.071$ ($R = 0.8342$). Both relationships were significant, but the correlation between forward bending and uniaxial compression was not strong, while strength was lower under forward bending than under uniaxial compression according to the Friedman multiple comparison test ($P = 0.00017$).

Conclusion. Strength under forward bending correlated significantly to that under uniaxial compression, but the correlation was not strong. Therefore, in osteoporotic patients, both uniaxial compression and forward bending should be assessed to evaluate fracture risk in daily living using a CT-based FE method.

Key words: vertebral fracture, osteoporosis, fracture strength prediction, nonlinear finite element analysis, fracture site. **Spine 2009;34:1464–1469**

From the *Department of Orthopaedic Surgery, University of Tokyo, Tokyo, Japan; and †Department of Orthopaedic Surgery, Tokyo Metropolitan Geriatric Medical Center, Tokyo, Japan.

Acknowledgment date: June 17, 2008. Revision date: January 17, 2009. Acceptance date: January 19, 2009.

The manuscript submitted does not contain information about medical device(s)/drug(s).

No funds were received in support of this work. No benefits in any form have been or will be received from a commercial party related directly or indirectly to the subject of this manuscript.

Address correspondence and reprint requests to Isao Ohnishi, MD, PhD, Department of Orthopaedic Surgery, School of Medicine, Tokyo University, 7-3-1 Hongo, Bunkyo-ku, Tokyo 113-0033, Japan; E-mail: ohnishii-dis@h.u-tokyo.ac.jp

Osteoporosis is a disease characterized by low bone mass and microarchitectual deterioration of bone tissue, leading to enhanced bone fragility and a resulting increase in fracture risk.[1] Osteoporotic vertebral fracture is common in the elderly, representing a serious event causing reduced activity or bedridden status with high mortality and morbidity rates.

Osteoporotic vertebral fractures occasionally occur slowly and asymptomatically and tend to be overlooked by clinicians. Such fractures seem to be caused by loading on the spine during activities of daily living that exceed the vertebral strength of the osteoporotic individual.[2] The most common type of vertebral fracture is reportedly wedge-shaped fracture[3,4] caused by axial and bending loads.[5,6] To assess the strength of osteoporotic vertebrae, evaluating vertebral strength under loading as experienced during daily living is important, particularly forward bending. Bone densitometry techniques can neither predict differences in bone strength with changing load direction nor identify sites at risk of fracture. Finite element models (FEM) based on data from quantitative computed tomography may predict vertebral strength more accurately because geometry, architecture, and heterogeneous mechanical properties of the bone are assessed. We have previously reported that vertebral strength could be predicted accurately using a computed tomography (CT)-based nonlinear FE method.[7] This method can also be used for *in vivo* assessments of vertebral strength.[8] Once accuracy has been established, various simulations will be able to be used in other situations by changing the direction and/or site of loading. If we could create a patient-specific CT-based nonlinear FE model of the vertebral body and strengths could be predicted under loading conditions simulating common activities of daily living, this would provide an extremely useful tool in clinical practice. On this background, we focused on the use of simulated loading conditions that are commonly encountered during activities of daily living. The purpose of the present study was to evaluate differences in predicted fracture strength of vertebral bodies among different loading conditions occurring during activities of daily living. Based on these analyses, we may be able to determine whether multiple loading conditions are necessary to evaluate vertebral fracture risk in osteoporotic persons.

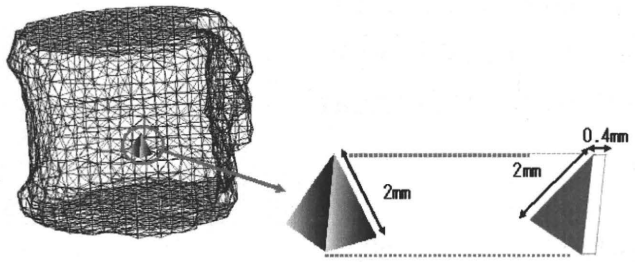

Figure 1. A FEM of a whole vertebral body. Trabecular bone was simulated using 2-mm tetrahedron elements, and the cortical shell was modeled using 2-mm triangular plates with a thickness of 0.4 mm. This model consisted of 4437 tetrahedral elements and 2518 triangular shell elements on average.

■ Materials and Methods

Subjects comprised 41 female patients (mean age, 69.4 years; range: 51–88 years) who could walk, visited the outpatient clinic of the Department of Orthopedic Surgery at the University of Tokyo between 2005 and 2007 and were diagnosed as postmenopausal osteoporosis according to the guidelines for prevention and treatment of osteoporosis as proposed by the Japanese Society of Osteoporosis (2006 ed.). No subjects had any previous history of disease or use of drugs affecting bone metabolism. The second lumbar vertebra (L2) was examined in these patients, and subjects with previous L2 fracture were excluded. With ethics committee approval, CT of L2 was performed after obtaining informed consent from each patient. CT of L2 was obtained using a slice thickness of 2 mm[8] and a pixel width of 0.37 mm with an Aquilion system (Toshiba Medical Systems, Tokyo, Japan; 120 kV, 75 mAs, 512 × 512 matrix), as along with a calibration phantom (B-MAS200; Kyoto Kagaku, Kyoto, Japan) containing 5 hydroxyapatite rods (0, 50, 100, 150, and 200 mg/cm^3). Predicted strengths under forward bending and erect standing were compared with that under uniaxial compression and differences in strength were statistically analyzed.

Nonlinear FE Analysis

Quantitative computed tomography-based FE models of vertebrae were created using methods described previously.[7–9] Mechanical Finder software, developed by the authors,[7–9] was used to extract bone area and for FE analyses. CT data in digital imaging and communication in medicine format were transferred to the workstation (Endeavor Pro-1000; Epson Direct, Nagano, Japan), and bone area of the L2 vertebral body was extracted from each scan. FE mesh models were then generated using the advancing front method. An FE model was created with 2-mm tetrahedral elements. Triangular elements with a thickness of 0.4 mm were attached to the model surface. On average, there were 44,337 tetrahedral elements and 2517 triangular shell elements (Figure 1).

To allow for bone heterogeneity, mechanical properties of each element were computed from the Hounsfield unit value. Ash density of each voxel was determined from the linear regression equation created by values from the calibration phantoms. Ash density of each element was set as the average ash density of voxels contained in one element. Young's modulus and yield stress of each tetrahedron element were calculated from the equations proposed by Keyak *et al.*[10] Young's modulus of cancellous tissue in human vertebrae has been reported as 3.8 to 13.4 GPa[11–14]; the minimum Young's modulus of each triangular plate was set as 10 GPa. Poisson's ratio of each element was set at 0.4, as used in previous articles.[7,9]

A uniaxial compressive load with uniform distribution was applied on the upper surface of the vertebra, with all elements and all nodes of the lower surface completely restrained. Loading configurations for erect standing and forward bending as described by Pollintine *et al*[15] were modified and adopted for analysis, as these were the postures most frequently occurring in the activities of daily living. Pollintine *et al* divided the loading area on the endplate of the vertebral body into 3 parts: anterior; posterior; and facet joint. They reported ratios of load magnitude (anterior: posterior: facet) of 19:41:40 for erect standing and 59:38:3 for forward bending. We modified the load distribution on the endplate according to these findings, as our model excluded posterior elements such as pedicles, lamina, and facet joints. Load distribution was divided into 3 parts: anterior; middle; and posterior. The ratio of load magnitude for each part was assigned on the assumption that the middle part bore the average load magnitude of the anterior and posterior parts. Ratios were thus 19:31:41 for erect standing and 59:48:38 for forward bending. Load was applied on the upper end plate vertically and the lower end plate was fully restrained (Figure 2).

Nonlinear analysis was performed using the Newton-Raphson method with a postyield modulus of 0.05. The ratio of ultimate stress to yield stress was assigned as 0.8. The element crack in tension was defined as occurring when maximum principal stress exceeded element ultimate stress. However, in compression, we introduced both yield and failure. Yield in compression was defined as occurring when Drucker-Prager equivalent stress exceeded element yield stress. Element failure in compression was then defined as occurring when the negative value of maximum principal strain exceeded 10,000 microstrain. Fracture load was defined as the load when at least one element failed. Predicted fracture load in each of the erect standing and forward bend-

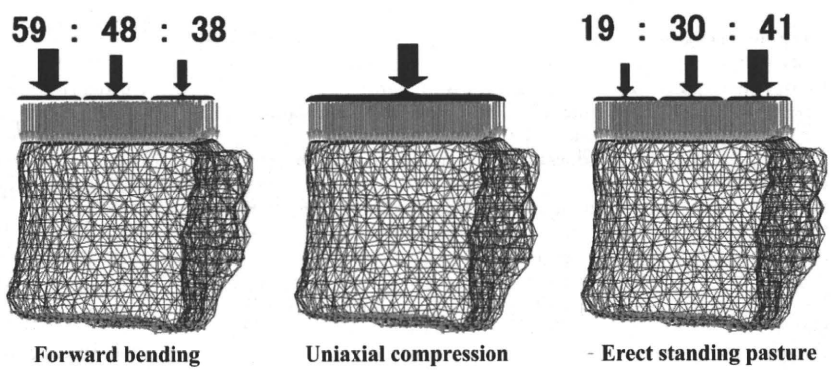

Figure 2. Load and boundary conditions in each model. Load distribution was divided into 3 parts: anterior; middle; and posterior. The ratio of load was thus 19:31:41 for erect standing and 59:48:38 for forward bending.

ing configurations was calculated and compared with that under uniaxial compression. To investigate differences among the 3 fracture loads from the different loading conditions, fracture load ratios were calculated. Fracture load ratio of forward bending (R_f) was represented as:

$$R_f = \frac{F_f}{F_u},$$

where F_f is predicted fracture load under forward bending and F_u is predicted fracture load under uniaxial compression.

Predicted fracture sites under each loading configuration were also identified. To analyze differences in distribution of fracture sites depending on differences in loading configuration, the whole vertebral body was divided into 3 parts in an anteroposterior direction and 3 parts in a cranio-caudal direction, for a total of 9 parts. Pearson correlation analyses were performed using StatView 5.0 (SAS Institute, Cary, NC). Paired analyses among the 3 groups were performed using the Friedman multiple comparison test. Analysis of differences in distributions of predicted fracture sites was performed using the χ^2 test for all loading conditions. Deviation of the distribution was analyzed by Ryan's method. Differences were considered significant for values of $P < 0.05$.

■ Results

Mean fracture load was 3062 N under uniaxial compression (range: 883–5688 N), 2918 N in erect standing (range: 883–5492 N), and 2693 N in forward bending (range: 883–5296 N). The linear regression equation relating fracture load in erect standing to that under uniaxial compression was expressed as y = 0.8912x + 19.332 (R = 0.9522, $P < 0.0001$) (Figure 3). Likewise, the equation relating forward bending to uniaxial compression was y = 0.7033x + 55.071 (R = 0.8342, $P < 0.0001$) (Figure 4). Mean fracture load was significantly lower in forward bending than under uniaxial compression ($P = 0.00017$).

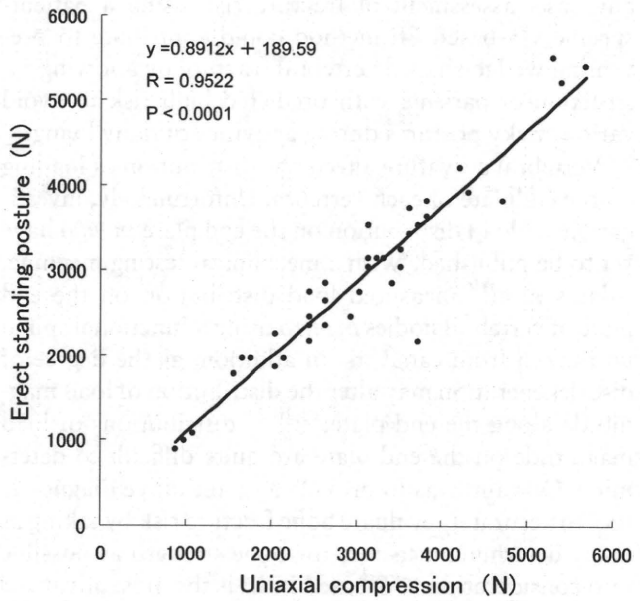

Figure 3. Predicted strengths under uniaxial loading and erect standing. A significant correlation was identified.

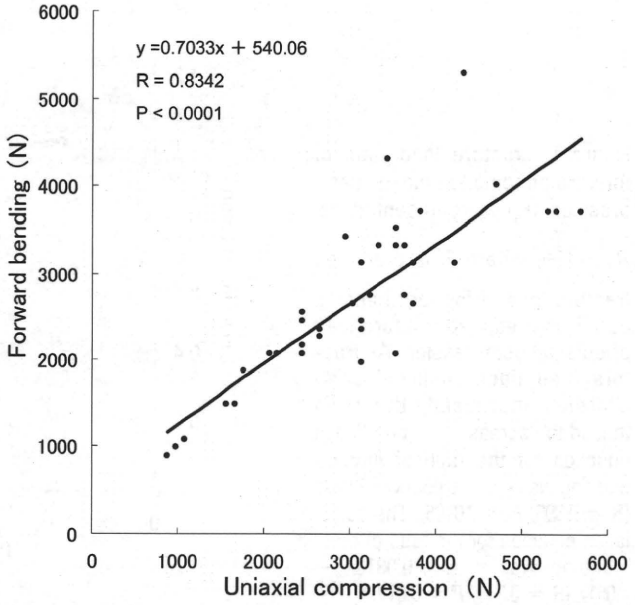

Figure 4. Predicted strengths under uniaxial loading and forward bending. A significant correlation was again identified.

In the evaluation of ratios of fracture load, as fracture load under uniaxial compression increased, fracture load ratio of both forward bending and erect standing tended to decrease (forward bending: y = −0.0527x + 1.0624, R = 0.393, $P = 0.0105$; erect standing: y = −0.0313x + 1.0617, R = 0.335, $P = 0.0137$) (Figure 5).

The distribution of predicted fracture sites is shown in Figure 6 for each of the loading configurations. In the cranio-caudal direction, fracture sites tended to be located in the upper third of the vertebral body under all loading configurations. In the anteroposterior direction, the antero-superior part was the most frequent predicted fracture site in forward bending, with76% of all sites. For both erect standing and uniaxial compression, the middle-superior part was the most frequent site (Figure 6). Under all loading conditions, significant differences existed in the distribution of predicted fracture sites. Using Ryan's multiple comparison, the antero-superior part was the most frequent fracture site in forward bending ($P < 0.005$). Under uniaxial loading, the middle-superior part was significantly more frequently affected than all parts except the antero-superior and postero-middle parts ($P < 0.005$). In erect standing, the middle-superior and postero-middle parts were significantly more frequent than the antero-middle and 3 inferior parts ($P < 0.005$) (Figure 7).

■ Discussion

Given the present results, fracture loads in erect standing and forward bending were highly correlated with those under uniaxial compression, with a correlation coefficient of 0.9522. However, the correlation between forward bending and uniaxial compression was moderate, with a coefficient of 0.8342. Strength in forward bending was significantly lower than uniaxial compression ac-

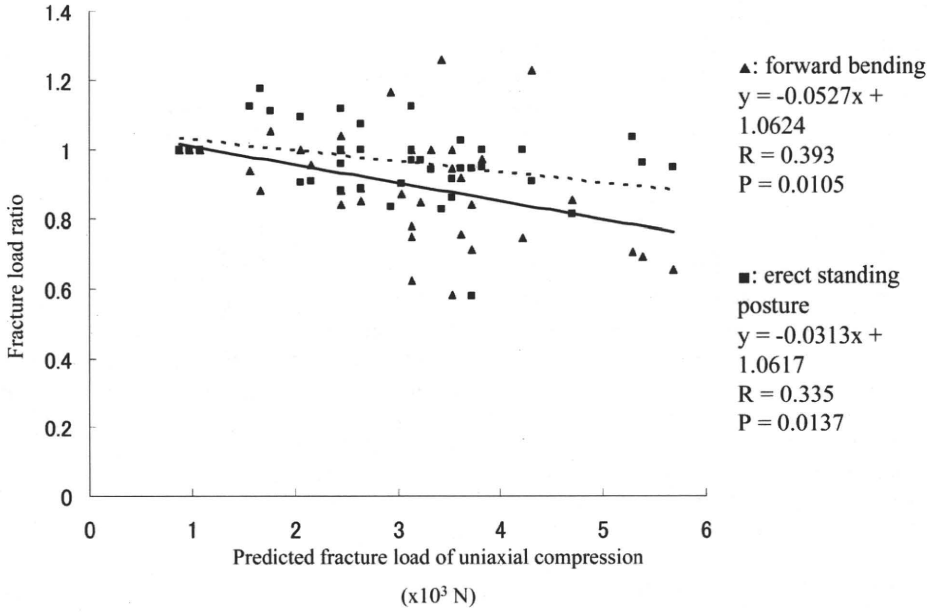

Figure 5. Fracture load ratio of forward bending to uniaxial compression (R_f) is represented as: $R_f = \frac{F_f}{F_u}$, where F_f is predicted fracture load of forward bending and F_u is predicted fracture load of uniaxial compression. As fracture load under uniaxial compression increased, the ratio tended to decrease. The correlation equation for the ratio of forward bending was $y = -0.0527x + 1.0624$ ($R = 0.393$, $P = 0.0105$). The correlation equation for the ratio of erect standing was $y = -0.0313x + 1.0617$ ($R = 0.335$, $P = 0.0137$).

cording to Friedman analysis. For fracture load ratio, as fracture load under uniaxial compression increased, the ratio of fracture load in forward bending to that under uniaxial compression tended to decrease. Therefore, when evaluating risk of vertebral fracture, assessment of predicted fracture load would need to be independently determined under each of the loading conditions to fully evaluate fracture risk during activities of daily living. Strength under uniaxial compression is clearly not representative of strengths under other loading configurations. If loading configurations under which the vertebrae are most vulnerable can be determined using CT-based FE analysis, atraumatic osteoporotic fractures may be able to be prevented by instructing patients to avoid such postures in activities of daily living.

Oda *et al*[16] reported that the most common deformity after atraumatic vertebral body fracture is a wedge-shaped deformity resulting from collapse of the anterior vertebral body. Wilke *et al*[17] reported that intradiscal pressure doubles with forward bending. A much larger compressive load is thus applied to the end plate during forward bending. Loading associated with forward bending was thought to be one of the factors causing wedge-shaped fracture, as the loading configuration that simulated forward bending in our study created identical

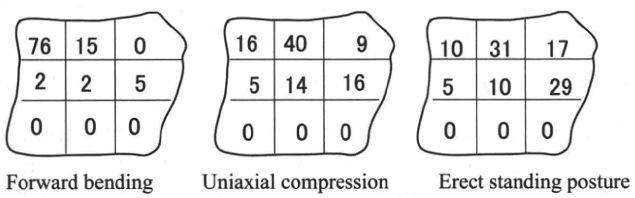

Figure 6. Distributions of predicted fracture sites under each of the loading configurations. Figures were expressed as percentages. Fracture sites tended to be located in the upper third of the vertebral body under all loading configurations. In forward bending, 76% of sites were present in the anterior third.

wedge-shaped deformities of the vertebral body. Conversely, under erect standing and uniaxial compression, predicted fractures occurred most frequently at the middle of the upper surface of the vertebral body and did not result in wedge-type fractures (Figure 8). Keller *et al*[18] reported that the anterior area of the vertebral body is both less dense and less strong than the posterior region. FE models that take accurate bone density distribution into consideration should thus be created to evaluate fracture risk under such conditions. In addition, to be clinically useful, simulation models should be based on loading conditions that can simulate common activities of daily living. So, based on the fact that strength under forward bending was significantly lower than under uniaxial compression, prediction of strength under forward bending should also be added for further assessment. In any case, assessment of fracture risk using a patient-specific CT-based FE method could contribute to preventing wedge-shaped vertebral fracture by allowing instruction of patients with predicted high risk to avoid various risky postures during activities of daily living.

Vertebral curvature affects the distribution of loading on the endplate of each vertebra. Unfortunately, investigations of load distribution on the end plate *in vivo* have yet to be published. With a mechanical testing machine, Adams *et al*[19] measured load distribution on the end plate of vertebral bodies *in vitro* using a functional spinal unit taken from cadavers. In addition, as the degree of disc degeneration may alter the distribution of load magnitude along the end plate,[18,20,21] distributions of load magnitude on the end plate are quite difficult to determine. Our aim was to provide a quantitative diagnostic tool to accurately evaluate bone fracture risk by taking as many determinant factors for bone strength as possible into consideration. CT-based FEM is the most advanced method to satisfy these demands. Our intention was not to provide a method to decide whether a bone in a certain

Forward bending

zone	1	2	3	4	5	6	7	8	9
1		0	0	0	0	0	0	0	0
2	0		0.00012	ns	ns	ns	0.0003	0.00079	0.00208
3	0	0.00012		ns	ns	ns	ns	ns	ns
4	0	ns	ns		ns	ns	ns	ns	ns
5	0	ns	ns	ns		ns	ns	ns	ns
6	0	ns	ns	ns	ns		ns	ns	ns
7	0	0.0003	ns	ns	ns	ns		ns	ns
8	0	0.00079	ns	ns	ns	ns	ns		ns
9	0	0.00208	ns	ns	ns	ns	ns	ns	

Uniaxial compression

zone	1	2	3	4	5	6	7	8	9
1		ns	ns	ns	ns	ns	ns	ns	ns
2	ns		0.00032	0.00001	0.00354	ns	0	0	0
3	ns	0.00032		ns	ns	ns	ns	ns	ns
4	ns	0.00001	ns		ns	ns	ns	ns	ns
5	ns	0.00354	ns	ns		ns	ns	ns	ns
6	ns	ns	ns	ns	ns		ns	ns	ns
7	ns	0	ns	ns	ns	ns		ns	ns
8	ns	0	ns	ns	ns	ns	ns		ns
9	ns	0	ns	ns	ns	ns	ns	ns	

Erect standing posture

zone	1	2	3	4	5	6	7	8	9
1		ns	ns	ns	ns	ns	ns	ns	ns
2	ns		ns	0.00121	ns	ns	0.00001	0.00002	0.00005
3	ns	ns		ns	ns	0.0015	0.00105	ns	ns
4	ns	0.00121	ns		ns	ns	ns	ns	ns
5	ns	ns	ns	0.0015		ns	ns	ns	ns
6	ns	ns	ns	ns	ns		0	0.00001	0.00004
7	ns	0.00001	0.00105	ns	ns	0		ns	ns
8	ns	0.00002	ns	ns	ns	0.00001	ns		ns
9	ns	0.00005	ns	ns	ns	0.00004	ns	ns	

Zone definition

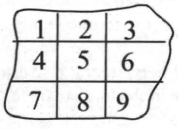

Figure 7. *P* values calculated using Ryan's method. Each zone was numbered; the antero-superior zone was numbered "1," middle-superior "2," and postero-superior "3." Middle row was numbered from the anterior column "4," "5," "6," and "9" for the postero-inferior zone.

patient would break under a certain mechanical environment. Instead, our approach involved the virtual extraction of a bone of interest from a patient and then examining that bone under virtual static mechanical testing. Predicted strength from this simulation may be far from accurate compared with that derived from more realistic simulations incorporating dynamic analyses or more realistic mechanics. Despite these limitations, CT-based FEM offers a far more advanced method to diagnose bone fragility than the prevailing clinically available bone densitometry. In the future, we intend to adopt more advanced simulation methods, including more realistic loading conditions that reflect the effects of spinal curvature and discs.

Another limitation was that our FE model did not include posterior elements. Previous studies that evaluated vertebral strength using a CT/FE model also excluded posterior elements.[22–24] This does not reflect actual loading configurations in activities of daily living. If the FE model could include posterior elements, simulation of the vertebral body under various loading conditions would be more realistic.

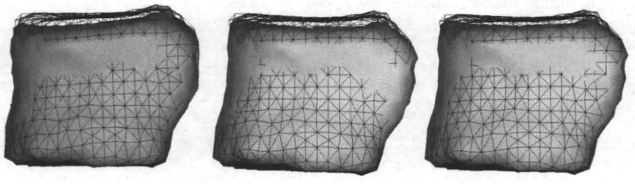

Forward bending Uniaxial compression Erect standing posture

Figure 8. Typical deformation of vertebral body under the 3 loading conditions magnified 10-fold. The anterior part collapsed under forward bending, resulting in wedge-shaped fracture. In uniaxial compression and erect standing, the middle upper part collapsed.

Analyses of fracture risks of vertebrae under loading condition simulating forward bending were performed by Bouxsein *et al*[25] by calculating "factor-of-risk" based on data on loads applied to vertebral bodies investigated by Schultz and Andersson.[26] However, Bouxsein *et al*[25] did not analyze predicted fracture sites.

Crawford[23] investigated rigidity and strain distributions of vertebrae using a linear FE method by inducing bending moment. The correlation between effective bending and axial rigidity of all vertebrae was reportedly R = 0.83. They concluded that axial properties were not necessarily strongly correlated with bending properties. In our study, although a different FE method was adopted from that of Crawford *et al*, the results were not contradictory between these studies. To the best of our knowledge, the present study is the only one to have investigated fracture strength of vertebrae under loading conditions simulating forward bending using a nonlinear FE method. Based on the present results, evaluation of fracture strength in patients with osteoporosis should be evaluated not only with uniaxial compression, but also using a forward-bending loading condition. At present, deriving a simple equation to help make a decision re-

garding treatment seems very difficult. We may need a prospective study in the near future to investigate which of the predicted strengths among the 3 loading conditions would result in the most accurate assessment of vertebral fracture risk in elderly individuals with osteoporosis. Assessment of vertebral strength using a CT-based FEM is clinically available and has been applied *in vivo*[8] and used for the evaluation of the efficacy of osteodynamic agents in treating osteoporosis.[27,28] In addition, investigations on the magnitude of stress at the bone-pedicle screw interface have been performed by creating a CT/FEM model of a lumbar vertebra with pedicle screws inserted.[29] CT/FEM has also been applied for analyzing vertebral strength after vertebroplasty using bone cement.[30] That study reported the effect of cement distribution on vertebral strength and stiffness. Accumulating basic and clinical data by conducting such studies will contribute to the creation of equations in the future that will allow surgeons to select suitable treatment options.

■ Key Points

- The fracture load in the forward bending was significantly lower than that in the uniaxial compression ($P = 0.00017$). The distribution of the predicted fracture sites tended to locate at the upper third of the vertebral body in all loading configurations.
- In osteoporotic patients, both uniaxial compression and forward bending should be assessed to evaluate fracture risk in daily living by using a CT-based FEM.

References

1. NIH Consensus Development Panel on Osteoporosis prevention, diagnosis, and therapy. *JAMA* 2001;285:785–95.
2. Melton LJ III, Chrischilles EA, Cooper C, et al. Perspective. How many women have osteoporosis? *J Bone Miner Res* 1992;7:1005–10.
3. Eastell R, Cedel SL, Wahner HW, et al. Classification of vertebral fractures. *J Bone Miner Res* 1991;6:207–15.
4. Melton LJ III, Lane AW, Cooper C, et al. Prevalence and incidence of vertebral deformities. *Osteoporos Int* 1993;3:113–9.
5. Granhed H, Jonson R, Hansson T. Mineral content and strength of lumbar vertebrae. A cadaver study. *Acta Orthop Scand* 1989;60:105–9.
6. Whealan KM, Kwak SD, Tedrow JR, et al. Noninvasive imaging predicts failure load of the spine with simulated osteolytic defects. *J Bone Joint Surg Am* 2000;82:1240–51.
7. Imai K, Ohnishi I, Bessho M, et al. Nonlinear finite element model predicts vertebral bone strength and fracture site. *Spine* 2006;31:1789–94.
8. Imai K, Ohnishi I, Yamamoto S, et al. In vivo assessment of lumbar vertebral strength in elderly women using computed tomography-based nonlinear finite element model. *Spine* 2008;33:27–32.
9. Bessho M, Ohnishi I, Matsuyama J, et al. Prediction of strength and strain of the proximal femur by a CT-based finite element method. *J Biomech* 2007;40:1745–53.
10. Keyak JH, Rossi SA, Jones KA, et al. Prediction of femoral fracture load using automated finite element modeling. *J Biomech* 1998;31:125–33.
11. Jensen KS, Mosekilde L, Mosekilde L. A model of vertebral trabecular bone architecture and its mechanical properties. *Bone* 1990;11:417–23.
12. Rho JY, Tsui TY, Pharr GM. Elastic properties of human cortical and trabecular lamellar bone measured by nanoindentation. *Biomaterials* 1997;18:1325–30.
13. Hou FJ, Lang SM, Hoshaw SJ, et al. Human vertebral body apparent and hard tissue stiffness. *J Biomech* 1998;31:1009–15.
14. Ladd AJ, Kinney JH, Haupt DL, et al. Finite-element modeling of trabecular bone: comparison with mechanical testing and determination of tissue modulus. *J Orthop Res* 1998;16:622–8.
15. Pollintine P, Dolan P, Tobias JH, et al. Intervertebral disc degeneration can lead to "stress-shielding" of the anterior vertebral body: a cause of osteoporotic vertebral fracture? *Spine* 2004;29:774–82.
16. Oda K, Shibayama Y, Abe M, et al. Morphogenesis of vertebral deformities in involutional osteoporosis. Age-related, three-dimensional trabecular structure. *Spine* 1998;23:1050–5; discussion 6.
17. Wilke HJ, Neef P, Caimi M, et al. New in vivo measurements of pressures in the intervertebral disc in daily life. *Spine* 1999;24:755–62.
18. Keller TS, Ziv I, Moeljanto E, et al. Interdependence of lumbar disc and subdiscal bone properties: a report of the normal and degenerated spine. *J Spinal Disord* 1993;6:106–13.
19. Adams MA, Pollintine P, Tobias JH, et al. Intervertebral disc degeneration can predispose to anterior vertebral fractures in the thoracolumbar spine. *J Bone Miner Res* 2006;21:1409–16.
20. Simpson EK, Parkinson IH, Manthey B, et al. Intervertebral disc disorganization is related to trabecular bone architecture in the lumbar spine. *J Bone Miner Res* 2001;16:681–7.
21. Kurowski P, Kubo A. The relationship of degeneration of the intervertebral disc to mechanical loading conditions on lumbar vertebrae. *Spine* 1986;11:726–31.
22. Buckley JM, Cheng L, Loo K, et al. Quantitative computed tomography-based predictions of vertebral strength in anterior bending. *Spine* 2007;32:1019–27.
23. Crawford RP, Keaveny TM. Relationship between axial and bending behaviors of the human thoracolumbar vertebra. *Spine* 2004;29:2248–55.
24. Crawford RP, Rosenberg WS, Keaveny TM. Quantitative computed tomography-based finite element models of the human lumbar vertebral body: effect of element size on stiffness, damage, and fracture strength predictions. *J Biomech Eng* 2003;125:434–8.
25. Bouxsein ML, Melton LJ III, Riggs BL, et al. Age- and sex-specific differences in the factor of risk for vertebral fracture: a population-based study using QCT. *J Bone Miner Res* 2006;21:1475–82.
26. Schultz AB, Andersson GB. Analysis of loads on the lumbar spine. *Spine* 1981;6:76–82.
27. Keaveny TM, Donley DW, Hoffmann PF, et al. Effects of teriparatide and alendronate on vertebral strength as assessed by finite element modeling of QCT scans in women with osteoporosis. *J Bone Miner Res* 2007;22:149–57.
28. Imai K, Ohnishi I, Matsumoto T, et al. Assessment of vertebral fracture risk and therapeutic effects of alendronate in postmenopausal women using a quantitative computed tomography-based nonlinear finite element method. *Osteoporos Int* 2008;19:383–4.
29. Chen SI, Lin RM, Chang CH. Biomechanical investigation of pedicle screw-vertebrae complex: a finite element approach using bonded and contact interface conditions. *Med Eng Phys* 2003;25:275–82.
30. Chevalier Y, Pahr D, Charlebois M, et al. Cement distribution, volume, and compliance in vertebroplasty: some answers from an anatomy-based nonlinear finite element study. *Spine* 2008;33:1722–30.

Evaluation of Bone Strength Using Quantitative Computed Tomography Based Finite Element Method - Clinical Application for the Diagnosis of Osteoporosis -

The Dept. of Orthopaedic Surgery, The University of Tokyo
Isao Ohnishi, Masahiko Bessho, Takuya Matsumoto, Masako Kaneko, Satoru Ohashi, Kazuhiro Imai, and Kozo Nakamura

The Computational Diagnostic Radiology and Preventive Medicine, The 22nd Century Medical Center, The University of Tokyo
Naoto Hayashi

The Dept. of Orthopaedic Surgery, Tokyo Metropolitan Geriatric Hospital
Fumiaki Tokimura

Tokyo Metropolitan Institute of Gerontology
Kim Hunkyung

Abstract

Fragility fractures are the most serious complication of osteoporosis and have been recognized as a major public health problem. It is essential to precisely quantify the strength of the fragile bone in order to estimate the fracture risk and plan preventive interventions. Quantitative computed tomography (QCT)-based finite element (FE) method (QCT/FEM) could possibly achieve precise assessment of the strength of the bone of interest. The purpose of the study was to create a simulation model that could accurately predict the strength and to apply this method in the wide range of clinical diagnosis in osteoporosis. We verified the accuracy of our model by load testing using fresh frozen cadaver specimens. The yield loads, fracture loads and principal strains of the prediction significantly correlated with those measured by load testing (r=0.941, 0.979, 0.963). FE analysis showed that the solid elements and shell elements in undergoing compressive failure were at the same region as the experimental fracture site.

QCT/FEM can predict vertebral compressive strength ex vivo. We aimed to assess vertebral fracture risk and alendronate effects on osteoporosis in vivo using QCT/FEM. Vertebral strength in 104 postmenopausal women was analyzed, and the discriminatory power for vertebral fracture was assessed cross-sectionally. Alendronate effects were also prospectively assessed in 33 patients with postmenopausal osteoporosis who were

treated with alendronate for 1 year. On the age and body weight adjusted logistic regression, vertebral strength had stronger discriminatory power for vertebral fracture (OR per SD change: 6.71) than areal bone mineral density (BMD) and volumetric BMD. The optimal point for the vertebral fracture threshold was 1.95 kN with 75.9% sensitivity and 78.7% specificity. At 3 months, vertebral strength significantly increased by 10.2% from baseline. The minimum principal strain distribution showed that the area of high fracture risk decreased. At 1 year, the density of the inner cancellous bone increased by 8.3%, while the density of the juxta-cortical area increased by 13.6%. QCT/FEM had higher discriminatory power for vertebral fracture than BMD and detected alendronate effects at 3 months. Alendronate altered density distributions, thereby decreasing the area with a high fracture risk, resulting in increased vertebral strength.

2009年4月30日発行・第17巻・第2号 通巻69号

日本骨粗鬆症学会雑誌
オステオポローシス ジャパン

Vol.17, No.2, 2009

Osteoporosis Japan

LIFE SCIENCE PUBLISHING

Osteoporosis japan

CT/有限要素法による椎体骨折リスクおよびアレンドロネート効果の評価

今井一博[1)]　大西五三男[2)]　山本精三[3)]
中村耕三[2)]

はじめに

骨粗鬆症の診断および治療効果判定は，従来エックス線写真・骨密度・骨代謝マーカー・新規骨折発生の抑制効果によって行われてきた。骨粗鬆症診療の目標は骨折リスクの評価および骨折の予防である。骨折リスクには骨脆弱化と転倒などの外傷があるが，近年，骨脆弱化には骨密度の低下だけではなく骨質の低下も関与しているとされ，「骨密度」と「骨質」を合わせた「骨強度」が新たな評価方法として注目されている。

有限要素法とは構造物に力が作用した時の反応をシミュレートして強度や力学特性を予測することが可能な解析法である。有限要素法による骨折予測は，おもに大腿骨近位部[1,2)]および椎体[3,4)]に対して行われてきた。しかしながら従来の有限要素法は，von Misesの最大剪断ひずみエネルギー説を採用し，0.2%の永久変形を降伏とするなど延性材料に使われる理論を用いているため，脆性材料である骨の破壊を適切に定義することができない，六面体要素を用いているため骨の複雑な曲面形状を構築できない，椎体の薄い皮質シェルを構築できず実際の強度に比較して著しく低く強度を予測する，といった問題があった。

骨強度および骨力学特性の解析に特化した評価法として，臨床用CT(computed tomography)データを使用したCT/有限要素法(MECHANICAL FINDER)が開発された。本法の特徴として，四面体要素を用いて複雑な曲面形状を構築，非線形解析により椎体の弾塑性を表現，海綿骨とは別に皮質シェルを構築，脆性材料に用いる理論を使用，骨折の定義が明確といった点があげられる。このCT/有限要素法により椎体強度および骨折部位を精度よく予測できることが新鮮死体標本での実証荷重試験によって示された[5)]。

CT/有限要素法を臨床応用するためには精度と放射線被曝が問題となる。骨梁構造を詳細に解析に反映して精度を向上させるためには，薄いスライス厚で高解像度のCT撮像を行い，細かい有限要素モデルを構築する必要がある。しかし現状の臨床用CT装置では，詳細で高解像度なCT撮像を行うと放射線被曝量が増大し，臨床応用するためには問題となる。有限要素モデルがどの程度のサイズであれば高精度に椎体強度および骨折部位を予測できるかを検証した結果，1mmサイズおよび2mmサイズでは精度が保たれていたが，3mmサイズでは精度が

Assessment of Vertebral Fracture Risk and Alendronate Therapeutic Effects by Computed Tomography Based Nonlinear Finite Element Method in Postmenopausal Women

Kazuhiro Imai：Department of Sports Medicine and Orthopaedic Surgery, Toshiba General Hospital, *et al.*

Key words： 有限要素法，骨粗鬆症，骨折リスク，治療効果

[1)]東芝病院スポーツ整形外科　[2)]東京大学医学部整形外科　[3)]虎ノ門病院整形外科

低下していた。臨床で1椎体をスライス厚2mmでCT撮像すると15～20スライスに相当し，組織荷重係数を0.2とすると放射線被曝量は3mSv程度となる。この被曝量は腰椎4方向のエックス線写真撮影の被曝量に相当するため，臨床応用可能と考えられた[6]。

本研究では，CT/有限要素法を用いて，閉経後女性における椎体骨折リスクおよび骨粗鬆症患者に対するアレンドロネートの効果を評価し，二重エネルギーエックス線吸収測定法(DXA：Lunar DPX-IQ)による骨密度(areal bone mineral density：aBMD)，CTによる骨密度(volumetric bone mineral density：vBMD)と比較・検討した。

1　対象と方法

1) 閉経後女性における椎体骨折リスクの評価

骨代謝・骨強度に影響する既往歴・薬剤歴がなく，第2腰椎に骨折などの病変がない閉経後女性129人を対象として，倫理委員会の承認のもと対象者の書面による同意を得て行った。外傷性椎体骨折既往者を除外した104人[平均年齢71.3歳：椎体骨折なし(非骨折群)75人，非外傷性椎体骨折あり(骨折群)29人]に対してDXAにより第2～4腰椎のaBMDを，CTにより第2腰椎のvBMDを測定した。また，CT/有限要素法により第2腰椎の単軸圧縮強度である椎体強度値を解析し，CT/有限要素法が椎体骨折リスク評価に有用かを検討した。非外傷性椎体骨折をスクリーニングする椎体強度値をreceiver operating characteristic(ROC)解析により求めた。また，ロジスティック回帰分析(年齢・体重を補正)にて骨折リスクのオッズ比を求めた。

2) 骨粗鬆症患者に対するアレンドロネート効果の評価

原発性骨粗鬆症の診断基準を満たし，骨代謝・骨強度に影響する既往歴・薬剤歴がなく，第2腰椎に骨折などの病変がない，アレンドロネート服用後に立位あるいは座位を30分以上保てる60歳以上の女性33人(平均年齢76.5歳)を対象とした。倫理委員会の承認のもと対象者の書面による同意を得て，5mg/日のアレンドロネートを投与した。DXAにより第2～4腰椎のaBMDをアレンドロネート投与開始前，および投与開始後6，12，18ヵ月時に測定した。第2腰椎のCTについては投与前，投与開始後3，6，12，18ヵ月時に撮影し，vBMDの測定およびCT/有限要素法による椎体強度値の解析を行った。また投与前および投与開始後3ヵ月時に尿中Ⅰ型コラーゲン架橋N-テロペプチド(NTx)を測定した。

2　結　　果

1) 椎体骨折リスクの評価[7]

対象者の閉経後女性104人のうち，非骨折群は平均年齢69.5±7.7歳(平均値±標準偏差)，平均身長150.6±5.1cm，平均体重51.5±7.3kgで，骨折群は平均年齢76.0±4.8歳，平均身長147.5±5.4cm，平均体重47.8±6.9kgであった。測定した平均aBMDは非骨折群が0.860±0.166g/cm^{2}で骨折群の0.719±0.209g/cm^{2}に比較して有意に大きく($p<0.05$：Mann-Whitney U検定)，平均vBMDは非骨折群が80.3±24.2mg/cm^{3}で骨折群の51.5±22.0mg/cm^{3}に比較して有意に大きく($p<0.0001$)，解析した平均椎体強度値は非骨折群が2.55±0.78kNで骨折群の1.59±0.51kNに比較して有意に高値を示した($p<0.0001$)。

ROC解析により検討した結果，非外傷性椎体骨折を効率よく判別できる至適カットオフ値は椎体強度値が1.95kNで体重の3.94倍の質量にかかる重量に相当し，感度75.9%・特異度78.7%であった。

対象者104人に対してロジスティック回帰分析にて年齢・体重を補正し骨折群の危険因子を評価したところ，1標準偏差の変化量に対するオッズ比はaBMDが1.83($p=0.0238$)，vBMDが3.57($p=0.0017$)，椎体強度値が6.71($p<0.0001$)と，椎体強度値の低下はaBMD・vBMDの低下より鋭敏な危険因子となっていた。椎体強度値のROC曲線下面積は0.822で，aBMD(面積0.713，$p=0.0010$)およびvBMD(面積0.767，

$p=0.0129$)より有意に高かった。

2) アレンドロネート効果の評価[7]

アレンドロネート投与開始前との変化率が追跡可能であったのは，投与期間12ヵ月までが33人，18ヵ月では6人であった。それぞれの平均変化率は，3ヵ月の椎体強度値が＋10.2%，6ヵ月が＋16.7%，aBMDでは＋3.7%，vBMDが＋5.1%，12ヵ月になると椎体強度値が＋26.9%，aBMDが＋7.5%，vBMDが＋8.8%であった。さらに，18ヵ月(6人)では椎体強度値が＋30.7%，aBMDが＋9.7%，vBMDが＋11.9%増加していた。

投与3ヵ月での椎体強度値変化率と尿中NTxの変化率は相関がなく($r=0.295$, $p=0.0955$)，投与12ヵ月での椎体強度値変化率とaBMD変化率には弱い相関($r=0.481$, $p=0.0046$)があった。CT/有限要素法による骨力学特性分析では，アレンドロネート投与前には圧縮ひずみが著しく骨折が生じやすいと考えられた領域において，投与後に圧縮ひずみの減少がみられた。また投与開始12ヵ月後には，椎体中央部の骨密度増加が8.3%($p=0.0013$)であったのに対し，皮質シェルを含む辺縁部では13.6%($p=0.0004$)の増加と，皮質近傍優位に薬剤効果がみられた。

3 考　　察

椎体骨折リスクの評価に関し，CT/有限要素法による椎体強度値はvBMDと同程度の識別能と報告されている[8]。一方，本研究では椎体強度値はaBMDおよびvBMDよりも有意に識別能が高かった。また，アレンドロネート効果の評価に関し，投与期間6ヵ月から18ヵ月のあいだでaBMDおよびvBMDは増加しているのに椎体強度値は減少したと報告されている[9]のに対し，本研究では投与期間18ヵ月においてaBMDおよびvBMDと同様ゆるやかではあるが，椎体強度値の増加が継続していた。

本研究が二つの先行研究と異なった結果である理由として，使用している有限要素モデルが異なることが一因と考えられる。先行研究では六面体要素であるのに対し，本研究は四面体要素を使用し，また本研究では先行研究にはない皮質シェルの構築を行っている。また，先行研究では延性材料に用いる理論および骨折定義を使用しているのに対し，本研究では引張に対しては脆性，圧縮に対しては弾塑性として，非線形解析にて降伏後の塑性も解析して骨の材料特性に基づき骨折の定義を行った点も，結果の相違に影響を与えたものと考える[5]。

アレンドロネートは投与開始後2～3年で骨密度の増加および新規骨折発生の抑制が得られることが報告されているが，臨床の場では投与開始後1年以内の，より早期に薬剤治療効果を知りたいという要求がある。本研究ではCT/有限要素法による椎体強度値はaBMD・vBMDより早期の投与開始後3ヵ月でアレンドロネートの効果判定に有用であった。また投与開始後18ヵ月間にわたり継続して椎体強度値の増加がみられた。

椎体強度値と尿中NTxの変化率に相関がないことより，椎体強度値は骨代謝を反映していないことが示唆された。一方，椎体強度値とaBMDの変化率には弱い相関があり，椎体強度値は骨密度を反映することが示唆された。またCT/有限要素法は骨密度に加え密度分布の変化を評価し，皮質近傍優位にアレンドロネート効果がみられていた。アレンドロネートの効果として皮質近傍の密度が増加するような密度分布の変化が生じ，圧縮応力の集中が軽減して圧縮ひずみ分布が改善し，椎体強度が増加したと考えられた。

アレンドロネートの皮質骨に対する効果としては，腸骨の微小血管造影法による評価でコントロール群と比較して石灰化度が皮質骨で9.3%，海綿骨で7.3%増加し，腸骨皮質骨で二次石灰化の延長があったと報告されている[10]。また腸骨の形態計測で，皮質骨中の多孔度が46%減少したと報告されている[11]。本研究では椎体において皮質シェル近傍優位に密度が増加していたが，骨微細構造について検討していない。腸骨皮質骨で報告されている二次石灰化の延長および多孔度の減少が椎体においても生じ

ているかについては，今後，組織学的検討，形態計測，マイクロCTなどによる評価が必要である。

また，骨リモデリングはマイクロダメージ，ひずみ，ひずみエネルギー密度に応答して生じるが，本研究ではアレンドロネートが圧縮ひずみやひずみエネルギー密度が大きい部位に直接作用しているわけではなく，皮質近傍の骨密度の増加により，結果として圧縮ひずみが軽減していた。アレンドロネートがどのパラメータに応答して作用するかは依然不明であり，今後の課題である。

骨粗鬆症診療におけるCT/有限要素法の役割として，骨強度を反映する要素のうち骨密度，密度分布，立体構造を評価できる点があげられるが，今後，CT/有限要素法とCT/有限要素法で評価できない骨代謝，骨微細構造の評価を組み合わせることにより，骨折リスク判定基準値の設定，骨粗鬆症治療薬剤効果の骨力学特性からの検証などに応用されることが期待される。

文　献

1) Keyak JH, Rossi SA, Jones KA, Skinner HB. Prediction of femoral fracture load using automated finite element modeling. J Biomech 1998;31:125-33.
2) Cody DD, Gross GJ, Hou FJ, Spencer HJ, Goldstein SA, Fyhrie DP. Femoral strength is better predicted by finite element models than QCT and DXA. J Biomech 1999;32:1013-20.
3) Silva MJ, Keaveny TM, Hayes WC. Computed tomography-based finite element analysis predicts failure loads and fracture patterns for vertebral sections. J Orthop Res 1998;16:300-8.
4) Crawford RP, Cann CE, Keaveny TM. Finite element models predict *in vitro* vertebral body compressive strength better than quantitative computed tomography. Bone 2003;33:744-50.
5) Imai K, Ohnishi I, Bessho M, Nakamura K. Nonlinear finite element model predicts vertebral bone strength and fracture site. Spine 2006;31:1789-94.
6) Imai K, Ohnishi I, Yamamoto S, Nakamura K. *In vivo* assessment of lumbar vertebral strength in elderly women using computed tomography-based nonlinear finite element model. Spine 2008;33:27-32.
7) Imai K, Ohnishi I, Matsumoto T, Yamamoto S, Nakamura K. Assessment of vertebral fracture risk and therapeutic effects of alendronate in postmenopausal women using a quantitative computed tomography-based nonlinear finite element method. Osteoporos Int 2009;20:801-10.
8) Melton LJ 3rd, Riggs BL, Keaveny TM, Achenbach SJ, Hoffmann PF, Camp JJ, et al. Structural determinants of vertebral fracture risk. J Bone Miner Res 2007;22:1885-92.
9) Keaveny TM, Donley DW, Hoffmann PF, Mitlak BH, Glass EV, San Martin JA. Effects of teriparatide and alendronate on vertebral strength as assessed by finite element modeling of QCT scans in women with osteoporosis. J Bone Miner Res 2007;22:149-57.
10) Boivin GY, Chavassieux PM, Santora AC, Yates J, Meunier PJ. Alendronate increases bone strength by increasing the mean degree of mineralization of bone tissue in osteoporotic women. Bone 2000;27:687-94.
11) Roschger P, Rinnerthaler S, Yates J, Rodan GA, Fratzl P, Klaushofer K. Alendronate increases degree and uniformity of mineralization in cancellous bone and decreases the porosity in cortical bone of osteoporotic women. Bone 2001;29:185-91.

ISSN 0919-0507

Osteoporosis Japan
オステオポローシス ジャパン

2009 Vol.17 Suppl.1

第11回日本骨粗鬆症学会
骨ドック・健診分科会
プログラム抄録号

The 11th
Annual Meeting of
Japan Osteoporosis Society
2009 NAGOYA

会期：2009年10月14日～16日
会場：名古屋国際会議場
会長：白木正孝 成人病診療研究所 所長

LIFE SCIENCE PUBLISHING

102 CT／有限要素法による大腿骨近位部の骨強度評価－検者内･検者間解析信頼性、解析再現性について－

東京大学　医学部　整形外科
別所　雅彦、大西五三男、松本　卓也、金子　雅子、
大橋　　暁、飛田　健治、松山順太郎、中村　耕三

【目的】骨粗鬆症に対する薬剤の治療効果判定を早期かつ正確に行うためには、精度や再現性が高い診断法を用いる必要がある。CT/ 有限要素法の正確性を検証する実証試験では、骨折荷重の解析値と実験値との相関は、r＝0.97 と高かかった（Bessho et al., 2007）。本研究の目的は、骨粗鬆症患者の大腿骨近位部を対象とし、CT/ 有限要素法による骨強度予測評価法の検者間・検者内信頼性および再現性を評価することである。【方法】1. 検者間・検者内信頼性評価：未治療の原発性骨粗鬆症の女性患者 10 名（平均 75 歳）を対象に、倫理委員会の承認のもと患者の同意を得て、右大腿骨近位部の定量的 CT 撮影の撮影を行った。CT 画像を元に、2 名の整形外科医（検者 A、検者 B）が、CT/ 有限要素法を用いて予測骨折荷重を解析した。Feldman ら（2007）の方法を参考に、2 回予測骨折荷重の解析を行った。ただし、1 回目の解析から 3 週間以上おいて 2 回目の再解析を行った。信頼性の指標として、級内相関係数（ICC）を用いて検者内・検者間解析信頼性を評価した。2. 再現性評価：72 歳女性の新鮮凍結大腿骨標本大腿骨 1 本を対象として、設置位置を変えて 6 回ＣＴ撮影した。6 回分の各 CT 画像を検者 A が予測骨折荷重を解析し、その変動係数を算出した。【結果】検者 A の検者内解析信頼性は、ICC 0.924 であった。検者間解析信頼性は、ICC 0.913 であった。大腿骨標本を用いたで解析再現性について、平均予測骨折荷重は 3675N、標準偏差は 52.4N であり変動係数は 1.43%であった。【考察、結論】信頼性の評価として、Altman ら（1991）は級内相関係数について、0.61～0.81 を Good、0.81～1.00 を Very good とした。今回の我々の解析手法の信頼性は高いと考えられた。また、解析の再現性について Cody ら（2000）は、10 名のボランティアによる in vivo での再現性（変動係数）は、1.85%であった。先行研究の結果とほぼ同等であると考えられた。DXA の再現性は一般的に 1～3％程度と言われており、CT/FEM の解析再現性は同等であると考えられた。今後、薬剤効果判定への応用を進めていきたいと考える。

103 CT 有限要素法による大腿骨近位部の骨強度評価－年齢別骨強度値の作成と骨強度に影響する因子の解析－

東京大学　医学部　整形外科[1]、東京大学医学部附属病院 22 世紀医療センターコンピュータ画像診断学予防医学講座[2]
金子　雅子[1]、大西五三男[1]、別所　雅彦[1]、
松本　卓也[1]、大橋　　暁[1]、飛田　健治[1]、
中村　耕三[1]、林　　直人[2]

【目的】定量的 CT データをもとにした有限要素法（CT/FEM）を用いて、骨の形態や構造、および不均一な力学特性分布を考慮した骨強度の正確な定量予測が可能である。しかし、現状では強度値に関して年齢別の基準値がなく、今後、本法を実用化するためには、年齢別の基準データが必須である。本研究は、検診目的で撮像およびデータ保存された PET-CT の DICOM Data を用い、CT/FEM により、年齢別に検診者の骨強度値を作成した。また骨強度に影響する因子を予備的に解析した。【対象と方法】以下の研究に関しては東大病院の倫理委員会の承認のもと患者の同意を得て行った。東大病院検診部にて検診を受け、除外基準に該当しない 40 歳以上の男性 353 名（平均 54.6 歳　40 歳～87 歳）、40 歳以上の女性　181 名（平均 59 歳　40 歳～83 歳）を対象とした。CT（GE 横河メディカル Discovery ST Elite）で骨量ファントムとともに撮像した後に記録・保存された DICOM Data を用い大腿骨近位部の 3 次元有限要素モデルを作成した。荷重・拘束条件を立位条件と転倒条件の 2 条件とし、非線形解析を行った（Bessho et al. J Biomech 2006）。得られた骨強度値の各年齢に対する分布図を作成し、大腿骨近位部の骨強度に影響する因子として、身長、体重および喫煙を解析評価した。相関検定はピアソンの相関係数を用いた。【結論・考察】大腿骨近位部の骨強度値は、男性では立位条件および転倒条件ともに年齢に対して減少する傾向があったが、年齢と有意な相関はなかった。女性では、立位条件および転倒条件とも年齢に対し有意に減少した。さらに、5 歳ごとの年齢区分において、平均値、95%信頼区間で検定を行うと、男性では、年齢とともに減少はあるが有意な相関はなかった。女性では、年齢帯ごとに有意に減少した。男性、女性とも身長と体重は骨強度値と有意に相関し、低身長、低体重ほど骨強度は低かった。男性では、喫煙 vs 禁煙、非喫煙 vs 禁煙では有意差はなかったが、喫煙者と非喫煙者で有意な相関があり、喫煙者で骨強度が低かった。今後、症例数を増やし、年齢別骨強度基準値の作成とともにより多くの骨強度関連因子について評価を行う。

106 当院におけるFRAX™を用いた骨折リスク評価の検討

札幌清田整形外科病院
片平弦一郎、中野　智博

【目的】10年間の骨折リスクを算出するツールFRAX™がWHOより提唱され我が国でも臨床の場で使用可能となった。今回我々はFRAX™を用い当院の患者における骨折確率（主要な骨粗鬆症性、大腿骨近位部）の算出と治療介入の実際について検討した。また患者アンケートを実施しその関心度を調査した。
【対象および方法】対象は当院を新規受診し骨粗鬆症検査を行った264例（男性19例女性245例、平均年齢71.8才）で、FRAX™を用い10年間の骨折率を大腿骨頚部骨密度およびBMI（骨密度無し）で計算した。治療介入閾値とする骨折率は、主要な骨粗鬆症性骨折で10、15、20%、大腿骨近位部骨折で3.5%について検討した。患者アンケートは自記式で行った。
【結果】全症例中骨量減少症が16.3%、骨粗鬆症が52.3%であった。骨量減少症例の骨粗鬆症性骨折の確率は大腿骨頚部骨密度を使い計算すると12.9%で、骨密度を使わずBMIのみで計算すると15.0%であった。大腿骨近位部骨折の確率は骨密度を使うと4.1%で、BMIでは5.9%であった。骨粗鬆症例の骨粗鬆症性骨折の確率は骨密度を使うと18.9%、BMIでは23.4%であった。大腿骨近位部骨折の確率は骨密度を使うと6.2%、BMIでは10.0%であった。

骨粗鬆症例は全例治療介入され、治療介入閾値を骨粗鬆症性骨折で10、15、20%、大腿骨近位部骨折で3.5%に設定した場合の治療対象者の割合を検討した。骨密度を使って計算した場合、骨粗鬆症例の骨粗鬆症性骨折介入閾値10%、15%、20%では各々79.6%，59.1%、38.7%の患者が該当し（BMI使用では各々81.9%、66.7%、52.2%）、大腿骨近位部骨折介入閾値3%、5%では各々61.2%、37.6%が該当した（BMI使用では各々75.4%、59.4%）。骨量減少症例では、骨粗鬆症性骨折介入閾値10%、15%、20%で各々42.3%、23.1%、15.4%が、大腿骨近位部骨折介入閾値3%、5%で各々34.6%、19.2%が該当した。骨量減少症例で薬物開始基準に従い治療介入されたのは骨量減少症例の18.6%で、その症例の骨粗鬆症性骨折率は平均9.1%、大腿骨近位部骨折率は平均1.3%であった。
【まとめ】骨折リスクは骨密度で算出した確率がBMI単独で算出するよりも低値を示し、これらの骨折確率は年令依存的に増加した。骨量減少、骨粗鬆症例ともに骨密度を使わずBMI単独で算出した方が治療対象者の割合が多くなった。患者アンケート結果より、約9割が骨折する確率を知りたいと回答し、高齢者ほど骨折の確率が低くとも治療を開始したいと回答した。

107 CT/有限要素法を用いた脊椎椎体の日常生活における骨強度評価－骨粗鬆症治療効果判定への応用－

東京大学　医学部　整形外科[1]、
伊奈病院　整形外科[2]
松本　卓也[1]、大西五三男[1]、別所　雅彦[1]、
金子　雅子[1]、大橋　暁[1]、飛田　健治[1]、
石橋　英明[2]、中村　耕三[1]

【目的】脆弱性椎体骨折の多くは緩徐かつ無症候性に出現し、楔状変形を呈する。これは、日常生活動作における椎体への荷重負荷が椎体の強度を超えるために起こる。第10回本学会において、CT/有限要素法を用いて、患者固有の椎体の解析モデルを作成し、日常生活動作を模擬した荷重条件による強度評価を行った。結果として、前屈荷重における強度は、単軸荷重における強度よりも有意に低値であった。これをふまえ、本法を骨粗鬆症の治療効果判定に応用するため、荷重条件の相違が治療後の骨強度に与える影響を比較検討した。【対象と方法】対象は、未治療の原発性骨粗鬆症で第2腰椎に圧迫骨折のない女性患者12名、平均年齢68.9歳（51～86）。ラロキシフェン（60mg/day）内服による加療を行った。倫理委員会の承認のもと患者の同意を得て、内服開始直前と1年後に、尿中NTX測定、第2腰椎のDXA測定、第2腰椎の定量的CT撮影を行い、CTのDICOMデータを用いて有限要素法による強度解析を行った。荷重条件・拘束条件は、椎体上面を垂直圧縮し、椎体下面を完全拘束した単軸圧縮モデル（Imai, 2006）、および立位と前屈位における椎体への荷重負荷分布（Pollintine, 2004）を改変応用して傾斜荷重を負荷した立位荷重と前屈位荷重の各モデルについて各条件ごとに骨折強度を解析し比較検討した。【結果】内服開始後1年で、尿中NTXは平均27.7%減少、DXA法による第2腰椎の骨密度増加は、平均2.9%増加、有限要素法による予測骨強度の増加率は、単軸圧縮で平均11.3%であり、DXA法より有意に増加した。前屈・立位条件では各々9.3%、6.5%増加した。症例ごとに検討すると、荷重条件の相違により増加率が解離した症例があった。骨密度分布の変化は、終板や皮質骨シェルに隣接した部位の骨密度の増加が目立ったが、症例により増加する部位が異なった。【考察・結語】薬剤投与により骨密度が増加するが、症例により骨密度の増加部位に変化があるため、CT/有限要素法による予測骨折荷重の増加は荷重条件の相違により異なる。よって、骨粗鬆症における椎体の骨折リスクは、骨密度分布や骨形態、骨質などの骨強度だけでなく、椎体に負荷する荷重の方向によっても変化するため、日常生活動作における荷重方向を考慮した解析条件を設定する事により、より正確な骨折リスク評価となり得る。

09(XVIII)-98

CT•CAD/有限要素法解析を用いたLag screw刺入高位による大腿骨頸部の応力・ひずみの検討

○松本卓也[a]，大西五三男[a]，別所雅彦[a]，大橋暁[a]，金子雅子[a]，飛田健治[a]，中村耕三[e]

[a]東京大学医学部整形外科

Assessment of the Lag Screw Bone Interface Using a CT and CAD Based Finite Element Analysis

T. Matsumoto[a], I. Ohnishi[a], M. Bessho[a], S. Ohashi[a], M. Kaneko[a], K. Tobita[a], K. Nakamura[a]

[a] *Department of Orthopaedic Surgery, University of Tokyo, Tokyo, Japan*

The purpose of this study was to assess stress and strain at a lag screw and bone interface using computer-aided design (CAD) data for a lag screw and patient-specific 3-dimensional (3D) finite element (FE) analysis (FEA). FE models were created from 3 patients with different bone mineral density. Using CAD data for a compression hip screw system which was supplied by the manufacturer (Mizuho Co Ltd., Japan), 3D FE models of the proximal femur with lag screw and angle plate in place were constructed. The screw was inserted at the center of the femoral neck in the sagittal plane parallel to the axis. In the coronal plane, 4 different screw positions were created; just above the calcar femorale (CF); 5 mm, 10 mm, 15 mm proximal to CF individually. Linear FEA was conducted, and the minimum principal strain and equivalent stress were calculated for each of the screw height conditions. Analysis of minimum principal strain and equivalent stress showed that the high value area tended to widen in a patient with osteoporosis, and that the more proximally the screw was inserted, the area with high equivalent stress widened at CF. Therefore, in severely w patients, placement of screws must be carefully planned to avoid postoperative cut out after fixation.

Key ward: hip fracture, osteoporosis, finite element analysis

【背景・目的】

高齢者の骨脆弱性に起因する大腿骨近位部骨折の患者の問題は社会的・経済的な問題だけでなく、治療上の問題として早期手術が望まれる一方で、周術期のリスクを高める合併症がありジレンマの中で治療法の選択に迫られる。手術に際しても、重度の骨粗鬆症は、通常の術後経過においてインプラントのカットアウトを引き起こし、再手術を余儀なくされる場合がある。臼井らはCHSによる手術療法は整復が良好で、ラグスクリューの位置が良ければ早期全荷重歩行が可能であると報告しており、個々の患者においてインプラントを適正に設置するための術前計画と術後のカットアウトのリスクを精度高く評価が必要である。本研究では大腿骨頸部の強度を高精度で予測する有限要素法解析モデル[1]を応用し、患者固有の大腿骨近位部のCT dicomデータとインプラントのCADデータを用いた有限要素法線形解析で、インプラント刺入高位の相違による大腿骨頸部/インプラント周囲の応力・ひずみを解析し、術後の荷重歩行によるカットアウトの危険性を予測・評価することである。

【対象と方法】

症例は骨粗鬆症骨折例として大腿骨転子部骨折を受傷した83歳女性、骨粗鬆症非骨折例として未治療の原発性骨粗鬆症患者の66歳女性、非骨粗鬆症例として大腿骨骨髄炎後の30歳女性の3例。使用するインプラントは手術手技としてスクリュー位置を最初に設定しプレートを設置するCHSを選択し

た。各症例に対し健側の大腿骨近位部を 2mm slice で定量的 CT を撮影。QCT Pro を用いて大腿骨頚部の骨密度(vBMD)を計測。

有限要素モデル作成・解析のソフトウエアーに RCCM 社製 MECHANICAL FINDER を用いた。各症例につき CT 画像上で閾値処理し解析対象となる健側大腿骨近位部を抽出、3 次元構築し、大腿骨転子部骨折の観血的整復内固定術を模擬して、頸部から骨頭直下まで瑞穂医科工業製の CHS・lag screw を大腿骨頸部の前後方向では中央かつ頸部骨軸に平行に、冠状面で lag screw 位置が、頸部最遠位(calcar 直上)のもの、頸部最遠位から 5mm、10mm、15mm 近位に設置し、各々に plate を骨幹部に取り付けたモデルを作成した。(図 1)

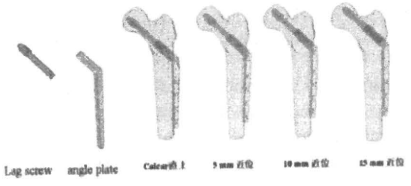

図 1 lag screw, angle plate とスクリュー刺入高位別の有限要素モデル

各有限要素モデルは大腿骨の海綿骨では 1〜4 ミリの四面体要素、皮質骨外層では 0.4mm 厚の正三角形要素の皮質シェルを構築、screw、plate の金属材料は 1〜4 ミリの四面体要素のみでシェル要素を用いなかった。各要素の材料特性は要素位置に対応する CT 値から骨密度を算出し、Keyak[2](1998)、Keller[3](1994)らの理論に基づいた不均一材料、金属材料は Ti6Al4V チタン合金のものを用い均一材料とした。金属材料と骨界面の境界条件は完全固着、screw と plate の境界はギャップ要素を用いた。荷重条件および拘束条件は、片脚に全体重をかけた体勢を模擬した条件を設定、980N の荷重をかけた。各有限要素モデルに対し線形解析を行い各症例について screw 高位別に相当応力、最小主ひずみ比較検討した。

【結果】

1.骨密度の比較

骨粗鬆症骨折例、骨粗鬆症非骨折例、非骨粗鬆症例の大腿骨頚部の vBMD は各々157.3 mg/cm3, 260 mg/cm3, 321.2 mg/cm3 であった。

2.最小主ひずみ分布

Screw 位置が calcar 直上より近位にあるほど大腿骨頸部における screw 周囲の最小主ひずみの絶対値および大腿骨頸部基部における相当応力が増加する傾向は若年例、骨粗鬆症例、骨折例の 3 例とも同様の傾向があった。しかし、応力・ひずみの絶対値が高い範囲は骨折例、骨粗鬆症例、若年例の順に少なくなる傾向にあった。(図 2)

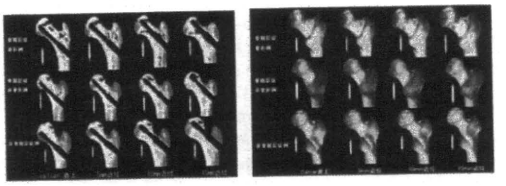

図 2 スクリュー刺入高位による最小主ひずみ分布(左)と相当応力分布(右)

【考察】

本研究結果より 3 例のうち骨密度が低いほど相当応力、最小主ひずみの絶対値ともに高くなる傾向にあるため、骨密度が低い症例ほどカットアウト予防のために刺入部位のより精確な決定を行う必要がある。大腿骨転子部骨折治療後の retrospective な臨床研究からカットアウトの予防のためにスクリューの設置位置や金属材料の相違、術後の荷重歩行について多くの報告がある。患者固有の解析モデルを作成できる本法を用いて、Gamma nail type などの種々のインプラントを検討することや骨折側のデータを利用して実際に骨折を整復・手術した状態の有限要素法モデルを作成し解析することによりより精細な術前計画や術後のリハビリ計画として発展させたいと考える。